Version of Record: https://www.sciencedirect.com/science/article/pii/S1096717623000757
Manuscript_cc46cf1cbc4b4d88404ebae243c4caaf

Engineering *Rhodosporidium toruloides* for Production of 3-Hydroxypropionic Acid from Lignocellulosic Hydrolysate

Di Liu[1,2†]*, Hee Jin Hwang[1,2†], Peter B. Otoupal[1,2,3†], Gina M. Geiselman[1,2,3], Joonhoon Kim[2,4], Kyle R. Pomraning[2,4], Young-Mo Kim[2,5], Nathalie Munoz[2,5], Carrie D. Nicora[5], Yuqian Gao[2,5], Kristin E. Burnum-Johnson[2,5], Oslo Jacobson[2,6,7], Samuel Coradetti[1,2,8], Jinho Kim[3,7], Shuang Deng[2,4], Ziyu Dai[2,4], Jan-Philip Prahl[2,6,7], Deepti Tanjore[2,,6,7], Taek Soon Lee[3,7], Jon K. Magnuson[2,3,4], John M. Gladden[1,2,3]*

[1]Biomanufacturing and Biomaterials Department, Sandia National Laboratories, Livermore, CA, USA;

[2]Agile BioFoundry, Department of Energy, Emeryville, CA, USA;

[3]DOE Joint BioEnergy Institute, Lawrence Berkeley National Laboratory, Emeryville, CA, USA;

[4]Energy and Environment Directorate, Pacific Northwest National Laboratory, Richland, WA, USA;

[5]Earth and Biological Sciences Directorate, Pacific Northwest National Laboratory, Richland, WA

[6]Advanced Biofuels and Bioproducts Process Development Unit, Lawrence Berkeley National Laboratory, Emeryville, CA, USA;

[7]Biological Systems and Engineering, Lawrence Berkeley National Laboratory, Berkeley, CA, USA;

[8]Present Address: Agricultural Research Service, United States Department of Agriculture, Ithaca, NY, USA

[†] These authors contributed equally.

*Correspondence: diliu@lbl.gov, jmgladden@lbl.gov

Abstract

Microbial production of valuable bioproducts is a promising route towards green and sustainable manufacturing. The oleaginous yeast, *Rhodosporidium toruloides*, has emerged as an attractive host for the production of biofuels and bioproducts from lignocellulosic hydrolysates. 3-hydroxypropionic acid (3HP) is an attractive platform molecule that can be used to produce a wide range of commodity chemicals. This study focuses on establishing and optimizing the production of 3HP in *R. toruloides*. As *R. toruloides* naturally has a high metabolic flux towards malonyl-CoA, we exploited this pathway to produce 3HP. Upon finding the yeast capable of catabolizing 3HP, we then implemented functional genomics and metabolomic analysis to identify the catabolic pathways. Deletion of a putative malonate semialdehyde dehydrogenase gene encoding an oxidative 3HP pathway was found to significantly reduce 3HP degradation. We further explored monocarboxylate transporters to promote 3HP transport and identified a novel 3HP transporter in *Aspergillus pseudoterreus* by RNA-seq and proteomics. Combining these engineering efforts with media optimization in a fed-batch fermentation resulted in 45.4 g/L 3HP production. This represents one of the highest 3HP titers reported in yeast from lignocellulosic feedstocks. This work establishes *R. toruloides* as a host for 3HP production from lignocellulosic hydrolysate at high titers, and paves the way for further strain and process optimization towards enabling industrial production of 3HP in the future.

Keywords: 3-hydroxypropionic acid, *R. toruloides*, malonyl-CoA reductase, lignocellulosic hydrolysate, 3-hydroxypropionic acid transporter

Introduction

3-hydroxypropionic acid (3HP) is one of the top 12 value-added chemicals proposed by the United States Department of Energy(Werpy and Petersen, 2004). It is an important platform precursor to a number of high-value commodity chemicals such as acrylic acid, 1,3-propanediol, methacrylic acid, propylene glycol. These chemicals are appealing industrial targets for bioplastics, metal lubricants, coatings and so on that have large market size. For example, 4.5 million metric tons of acrylic acid is made industrially from hydrocarbon-based propylene, accounting for a $7-10 billion market alone(Beerthuis et al., 2015). However, polypropylene is a heavily carbon-intensive feedstock, and more environmentally friendly alternatives are desirable(Zhao et al., 2017).

While multiple chemical synthesis routes have been proposed to produce 3HP, their feasibility for large-scale production is limited due to low yield, high cost of starting material, toxic or non-recyclable catalysts, and environmental incompatibility(della Pina et al., 2011). As an attractive alternative, microbial production of 3HP is 1) sustainable and environmentally friendly, 2) uses cheap feedstocks as substrates, and 3) has potentially high yields from a variety of metabolic pathways(Kumar et al., 2013). Therefore, methods to biologically synthesize 3HP have garnered significant attention for sustainable industrial production.

There are at least three main biological pathways for producing 3HP via the metabolites glycerol, β-alanine, and malonyl-CoA. The glycerol reduction pathway is used natively by organisms such as *Klebsiella pneumonia* to produce 3HP(Jiang et al., 2018; Li et al., 2016), and modification of this native pathway has resulted in one of the highest reported 3HP titers of 84 g/L from glycerol

as a feedstock (Li et al., 2016). Most of the studies on the glycerol pathway have used bacterial hosts and porting the glycerol route to eukaryotic hosts such as *Saccharomyces cerevisiae* is challenging due to the lack of cofactor vitamin B12(Borodina et al., 2015). As a result, most studies engineering heterologous production of 3HP in eukaryotic hosts have focused on the β-alanine and malonyl-CoA pathways(Ji et al., 2018). Researchers have successfully integrated the β-alanine pathway into *S. cerevisiae* to obtain 13.7 g/L titers of 3HP(Borodina et al., 2015).

One promising biosynthetic route for 3HP production is through the malonyl-CoA pathway since 1) it is a one-step pathway which is metabolically cost-effective, and 2) it has been widely adopted in various host species. This pathway has been successfully expressed heterologously to produce 3HP in *S. cerevisiae*(Chen et al., 2014; Kildegaard et al., 2015), *Escherichia coli*(Cheng et al., 2016; Lama et al., 2021; Rathnasingh et al., 2012), *Methylobacterium extorquens*(Yang et al., 2017a), *Synechocystis*(Wang et al., 2016), and *Schizosaccharomyces pombe*(Takayama et al., 2018). A critical enzyme in these studies is the malonyl-CoA reductase (MCR) originally involved in the carbon fixation pathway of the photosynthetic bacteria *Chloroflexus aurantiacus*, an organism capable of using CO_2 as its sole carbon source(Hügler et al., 2002). In *C. aurantiacus*, MCR performs a two-step reduction of malonyl-CoA to 3HP. The bifunctional enzyme contains an alcohol dehydrogenase N-terminus and aldehyde dehydrogenase C-terminus that perform the 2^{nd} and 1^{st} steps respectively (Fig. 1). The C-terminus has been demonstrated to be the rate-limiting step when expressed in *E. coli*, and 3HP titers were increased 270-fold when each domain was expressed independently(Liu et al., 2016, 2013).

The oleaginous basidiomycete *Rhodosporidium toruloides* is an attractive host for industrial scale production of many bioproducts(Park et al., 2018; Wen et al., 2020; Yaegashi et al., 2017). Not only does it readily co-consume the complex C5 and C6 sugar mixtures commonly derived from lignocellulosic biomass(Geiselman et al., 2020b; Osorio-González et al., 2019) and is tolerant to many inhibitors in the biomass hydrolysate(Hu et al., 2009), it can also grow to very high cell densities to over 100 g/L (Ageitos et al., 2011). *R. toruloides* has been engineered to produce various bioproducts from lignocellulosic feedstocks, including fatty alcohols up to 8 g/L (Fillet and Adrio, 2016; Liu et al., 2020; Schultz et al., 2022), indigoidine up to 18.0 g/L (Wehrs et al., 2019), and terpenes up to 2.6 g/L (Das et al., 2021; Geiselman et al., 2020a, 2020c; Kirby et al., 2021). *R. toruloides* has been found to exhibit a naturally high flux of acetyl-CoA into malonyl-CoA due to high expression of acetyl-CoA carboxylase (ACC)(Liu et al., 2009), thus making it a promising host for 3HP production via the malonyl-CoA pathway. Furthermore, the genetic engineering toolbox for manipulating this once-niche organism is rapidly becoming increasingly robust with the establishment of strong promoters(Nora et al., 2019) and advanced CRISPR-based DNA editing strategies(Jiao et al., 2019; Otoupal et al., 2019; Schultz et al., 2019).

Here we explore the production of 3HP in *R. toruloides*. We constructed the malonyl-CoA to 3HP pathway through expression of MCR from *C. aurantiacus* (MCR_{ca}). While expressing the full-length MCR_{ca} gene in *R. toruloides* failed to produce 3HP, expressing the N- and C- termini independently led to successful 3HP production with titers of 2.2 g/L. However, we observed significant consumption of 3HP subsequent to production. To improve 3HP production, we used a randomly barcode, random insertion library of *R. toruloides* and performed an RB-TDNAseq

experiment (Coradetti et al., 2017) to identify and delete genes involved in 3HP catabolism. We also conducted research to identify potential transporters that export 3HP. Coupled with media optimization, these strategies led to the production of 45.4 g/L titers of 3HP from lignocellulosic hydrolysate in a fed-batch bioreactor using glucose feed. Our study thus demonstrates one of the highest 3HP titers from the malonyl-CoA pathway in yeast from lignocellulosic feedstocks. This study further establishes *R. toruloides* as a promising host for the production of 3HP and other biofuels and bioproducts.

Materials and Methods

2.1 Plasmids and strains

WildType *Rhodosporidium toruloides* strain IFO0880 and its derivative with the *Ku70* gene deleted were obtained from our previous studies(Coradetti et al., 2018; Yaegashi et al., 2017) and used as base strains for this study. *Aspergillus pseudoterreus* strains used in this study were described previously(Pomraning et al., 2021).

Gene synthesis and plasmid construction were performed by Genscript (Piscataway, NJ). The gene encoding malonyl-CoA reductase from *C. aurantiacus* (MCR_{Ca}) was codon optimized for *R. toruloides* based on a custom IFO0880 codon usage table using the most frequently used codons. MCR_{Ca} was cloned intact as the full-length gene under the control of the forward direction of a strong, constitutively expressed bi-directional promoter "P9" from our previous study(Nora et al., 2019) (available as JPUB_013271 in the Joint BioEnergy Intitute's Public Registry website, accessible at https://public-registry.jbei.org/). Additionally, the gene was split into its N- and C-

termini based on a previous publication(Liu et al., 2016) and cloned under the control of the forward and reverse directions of promoter P9 respectively to generate strain "$MCR_{Ca\text{-}Split}$".

The MCR_{Ca} expression cassettes were then introduced into *R. toruloides* by targeted integration at the *CAR2* locus using LiAc transformation. All strains and plasmids used in this study are listed in Supplementary Table S1 and S2, and can be found on the Agile BioFoundry Registry website where they are available upon request (https://public-registry.agilebiofoundry.org/(Ham et al., 2012)).

2.2 Medium and culture conditions

Synthetic defined (SD) medium was made following manufacturers' guidelines with 1.7 g/L yeast nitrogen base (BD Biosciences, DF0919), 0.79 g/L complete supplement mix (Sunrise Science), and 100 g/L glucose. The pH was adjusted to 7.0 with NaOH. Strains were first cultivated overnight in Yeast Extract-Peptone-Dextrose (YPD) medium (BD Difco) at 30°C with 200 rpm shaking, which were subsequently inoculated into fresh YPD medium with a 1% (v/v) inoculum. Then the overnight cultures were inoculated into a fresh SD medium with a starting optical density at 600 nm wavelength (OD_{600}) measurement of 0.1. The cells were cultured for 3 days for further analysis. All productions were carried out in three or four biological replicates.

For nitrogen optimization, a single colony of $MCR_{Ca\text{-}Split}$ was inoculated into 10 mL YPD, supplemented with 100 µg/mL carbenicillin and 100 µg/mL cefotaxime. Cells were grown at 30°C with 200 rpm shaking for 24 hrs. Cells were next cultivated in media derived from corn stover biomass which was subjected to deacetylation and mechanical refining (DMR) processing of the biomass into hydrolysate(Chen et al., 2016). 500 µL culture was added to 9.5 mL of 16.7%

(v/v) DMR hydrolysate and mock DMR hydrolysate media with the indicated nitrogen sources and C:N ratios. DMR hydrolysate medium was made by diluting a concentrated DMR hydrolysate(Chen et al., 2016) to 100 g/L of total sugar (64.6 g/L glucose and 34.3 g/L xylose), with addition of 0.1 mM $FeSO_4$, 100 mM potassium phosphate (buffered to pH 5.6), 100 µg/mL carbenicillin, and 100 µg/mL cefotaxime. Mock hydrolysate medium is a SD medium containing the same glucose and xylose concentrations as the DMR hydrolysate medium, with addition of 0.1 mM $FeSO_4$, 100 mM potassium phosphate (buffered to pH 5.6), 0.79 g/L YNB without ammonium sulfate or amino acids, 1.7 g/L CSM, 100 µg/mL carbenicillin, and 100 µg/mL cefotaxime. Various elemental C:N ratios (by moles) were tested which includes 4:1, 8:1, 40:1 and 160:1. The nitrogen sources ammonium sulfate and urea were tested. Cells were grown at 30°C with 200 rpm shaking for 24 hrs. OD_{600} was measured and the culture was diluted for an OD_{600} of 0.1 in 1 mL using a 48-well FlowerPlate (m2p-labs) with flower-shaped baffles to support mixing, and sealed with a gas-permeable sealing film (Excel Scientific Inc). Cells were grown at 30°C with 930 rpm shaking and 70% humidity in a Multitron (Infors HT). Biological triplicates were used. Samples were taken between days 1 and 5 and were frozen at -20°C until further analysis. Samples were thawed, centrifuged at 1,504 × g for 3 minutes, and supernatant diluted 1:20 (v/v) into water. Samples were filtered with 0.2 µm filtration at 3,220 × g for 5 minutes. Sugar and 3HP were quantified via HPLC.

For minimal media experiments, minimal medium was prepared using 6.7 g/L yeast nitrogen base without amino acids (BD Difco) supplemented with 0.79 g/L CSM powder (Sunrise Science Products) and adjusted to a starting pH of 6.0. This medium was supplemented with either 10 g/L glucose, 0.5% (v/v) 3HP (TCI chemicals), or both.

For strain stability test, single colonies of MCR-ALD6-g2945 were inoculated into YPD media. For the ensemble level test, overnight YPD cultures were inoculated into DMR8U pre-adaptation media. The overnight cultures from the pre-adapted media were then inoculated into DMR8U media at an initial OD of 0.1. We then inoculated cultures grown in DMR8U media at day 1, 2 and 3 into fresh DMR8U media, and collected samples for 3HP analysis after 3 days. For the individual cell level test, overnight YPD cultures were inoculated into DMR8U media with an initial OD of 0.1. The cultures were grown for 3 days before sample collection and plating on YPD. Colonies from the YPD plate were inoculated into YPD media, and the overnight YPD media were inoculated into DMR8U media with an initial OD of 0.1. The cultures were grown for 3 days before sample collection. All production were carried out in three biological replicates.

2.3 Transformation of R. toruloides

Heterologous DNA was introduced into the *R. toruloides* genome using a modified version of lithium acetate (LiAc) transformation. *R. toruloides* base strains were streaked onto YPD plates, individual colonies were selected, and grown in 10 mL YPD overnight at 30°C with 200 rpm shaking. The following afternoon, cultures were diluted to an OD_{600} such that they would reach an OD_{600} of 0.8 the following morning, assuming a growth rate of 0.3 hr^{-1}. Cultures for transformation were pelleted at 4,000 × g for 5 minutes and washed twice with H_2O and twice with 150 mM LiAc (Sigma-Aldrich). Pellets were resuspended in 240 µL 50% (wt/vol) PEG 4000 (Sigma-Aldrich), 54 µL 1.0 M LiAc, 10 µL salmon sperm DNA (Thermo Fisher), and 56 µL of transforming DNA (approximately 1 mg of plasmid DNA linearized with PvuII). Cells were incubated at 30°C for 1 h, supplemented with 34 µL of DMSO (Sigma-Aldrich), and

incubated at 37°C for 5 min. Cells were centrifuged, washed once with YPD, and grown overnight in 2 mL YPD. Overnight cultures were plated on YPD supplemented with the appropriate antibiotic and grown for 2-3 days at 30°C.

2.4 Analytical methods

Cell density was measured by the absorbance at 600 nm wavelength (OD_{600}) (SPECTRAmax Plus, Molecular Devices). For quantification of extracellular metabolites including glucose, glycerol, xylose and 3HP, a high-performance liquid chromatography (HPLC) system (Agilent) equipped with an HPX-87H column (Bio-Rad) and a refractive index detector (RID, Agilent) was used. The autosampler, column and RID temperature were maintained at 4°C, 65°C and 45°C, respectively. The mobile phase was 5 mM sulfuric acid solution at a flow rate of 0.6 mL/min. All samples were filtered through a 0.22 µm membrane filter (VWR centrifugal Filter) before injection of 10 µL of filtered samples.

2.5 Deletion of 3HP consumption pathway

The putative gene responsible for 3HP consumption, *RTO4_8975*, was deleted using CRISPR-Cas9 to introduce indels causing a frameshift as we previously outlined(Otoupal et al., 2019). Plasmid ABF_010410 was linearized with PvuII restriction enzyme digestion (ThermoFisher) and transformed into WT IFO0880 as described in Section 2.3. Colony PCR followed by Sanger Sequencing (Azenta) was performed to identify successful frameshifts as outlined in Supplementary Fig. 2.

To confirm abated 3HP consumption, WT, $MCR_{Ca\text{-}Split}$, and WT Δ*RTO4_8975* were streaked onto YPD plates and cultivated at 30°C for 2 days. Three biological replicates of each strain

were inoculated into 5 mL YPD and grown for 2 days at 30°C with 200 rpm. Cultures were diluted 1:1000 (v/v) into 1 mL minimal media containing 0.5% (v/v) 3HP and supplemented with or without 10 g/L glucose as the carbon source and cultivated for 6 days at 30°C. OD_{600} measurements were sampled at day 2, and 3HP concentrations were subsequently measured as previously described at the end of the experiment.

2.6 Bioreactor fermentation

For bioreactor fermentations in the Ambr® 250 system, YP20D medium was made with 10 g/L yeast extract, 20 g/L Bacto-tryptone and 200 g/L glucose supplemented with 100 µg/mL carbenicillin and 100 µg/mL cefotaxime. 3HP production in $MCR_{Ca\text{-}Split}$ was examined using a fed-batch Ambr® 250 system (Sartorius AG., Goettingen, Germany). Fermentation was performed at 30°C with agitation at 400 rpm. A lower limit pH of 5 was set, with automatic feeding of 2 N NaOH to cultures falling below this limit. Foaming was suppressed by adding 1% (v/v) antifoam in water (Antifoam 204, Sigma). 150 mL YP20D medium was inoculated with an overnight culture in YPD at an initial OD_{600} of 0.1. Culture samples of 2 mL were collected at a series of time points every 24 hrs to monitor cell density, sugar consumption, and 3HP and glycerol production. A 600 g/L glucose solution was used to bring up glucose concentrations to 50 g/L at day 3 and day 4 when they were exhausted in the medium.

For 3HP production in the fed-batch 2 L bioreactor, MCR-ALD6-g2945 strain was inoculated in YPD with two antibiotics (100 µg/mL carbenicillin and 50 µg/mL hygromycin B) and grown for 2 days. For the adaptation, the overnight culture was inoculated 1% (v/v) into fresh 5 mL 50% (v/v) diluted modified DMR8U medium and grown overnight. The final seed culture was inoculated into a 250 mL baffled flask containing 50 mL 50% (v/v) diluted modified DMR8U

medium at 30°C and 200 rpm for 12 h. The cell culture was inoculated at an initial OD_{600} of 1.0 in a 2 L bioreactor (Biostat B, Sartorius, Germany) containing 1 L modified DMR8U medium. The modified DMR8U medium contains DMR hydrolysate with 120 g/L total sugar, 16 g/L urea, 10.7 g/L K_2HPO_4, 5.2 g/L KH_2PO_4, 10 mM $MgCl_2$, 1 mL of trace metal solution, 1 mL of vitamin solution and antibiotics (100 µg/mL carbenicillin and 50 µg/mL hygromycin B). The trace metal solution contained: 4.5 g/L $CaCl_2$•$2H_2O$, 4.5 g/L $ZnSO_4$•$7H_2O$, 3 g/L $FeSO_4$•$7H_2O$, 1 g/L H_3BO_3, 1 g/L $MnCl_2$•$4H_2O$, 0.4 g/L Na_2MoO_4•$2H_2O$, 0.3 g/L $CoCl_2$•$6H_2O$, 0.1 g/L $CuSO_4$•$5H_2O$, 0.1 g/L KI, and 15 g/L EDTA. The vitamin solution contained 50 mg/L biotin, 200 mg/L 4-aminobenzoic acid, 1 g/L nicotinic acid, 1 g/L Ca-pantothenate, 1 g/L pyridoxine-HCl, 1 g/L thiamine-HCl, and 25 g/L myo-inositol(Jinho Kim et al., 2021). The dissolved oxygen (DO), airflow, and temperature were set to 30 %, 2 VVM (volume of air per volume of liquid per minute), and 30°C, respectively. The pH was left uncontrolled. To produce 3HP in the fed-batch fermentation, 600 g/L glucose feeding stock solution was added manually when the residual glucose concentration dropped below 20 g/L in the medium to maintain 50-100 g/L glucose in the medium. The residual glucose was measured using a glucose meter (CVS Health) and HPLC as described previously(Jinho Kim et al., 2021).

2.7 Proteomic and metabolomic analysis

Samples for differentially expressed metabolites were collected during the Ambr® 250 run. Briefly, six OD_{600} samples were taken on day 1 and day 4, washed once with water and pelleted for 5 minutes at 4,000 rpm. Strains to explore metabolic shifts in different nitrogen sources were cultured in 48-well FlowerPlates. Six OD_{600} samples were also collected on day 3 and day 5, washed once with water and pelleted for 5 minutes at 4,000 rpm. All cell pellets were flash

frozen with liquid nitrogen and stored at -80°C until further analysis. Extraction of metabolites and proteins, as well as global proteomic and metabolomic analysis were performed with methods published in previous studies(Joonhoon Kim et al., 2021).

2.8 Fitness analysis with RB-TDNAseq

Fitness analysis was performed as described in a previous study(Coradetti et al., 2018). Briefly, three aliquots of the random insertion mutant pool of *R. toruloides* were thawed on ice and recovered in 100 mL YPD (BD Difco, 242820) for two generations (OD_{600} 0.2 to OD_{600} 0.8). A 10 mL of each starter culture was pelleted and frozen as an initial "time 0" sample. The remaining cells were pelleted 5 minutes at 4,000 RCF, washed twice with water and inoculated at OD_{600} 0.1 in 50 mL SD media with or without 76 mM KH_2PO4 (Sigma Aldrich) and 24 mM K_2HPO4 (Sigma Aldrich), supplemented with 1% (w/v) carbon source at pH 5.0 to 7.0 (as indicated). Cultures were grown to OD_{600} between 5 to 10 (approximately 20 to 50 hrs depending on carbon source) at 30°C, 200 rpm in baffled flasks (DWK Life Sciences). 10 mL samples were pelleted and frozen for DNA extraction. DNA extraction, barcode amplification, and sequencing was performed as described in Kim et al(Joonhoon Kim et al., 2021). The whole dataset is provided in Additional File 1.

2.9 RNA-seq analysis of A. pseudoterreus strains

For shake-flask experiments, 1E6 *A. pseudoterreus* spores were inoculated in 50 mL production medium B (Riscaldati et al., 2000) (supplemented with various carbon sources, 2.36 g/L $(NH_4)_2SO_4$, 0.11 g/L KH_2PO_4, 2.08 g/L $MgSO_4.7H_2O$, 0.13 g/L $CaCl_2.2H_2O$, 74 mg/L NaCl, 1.3 mg/L $ZnSO_4.7H_2O$, 0.7 mg/L $MnCl_2.4H_2O$, 5.5 mg/L $FeSO_4.7H_2O$, 0.2 mg/L $CuSO_4.5H_2O$,

adjusted to pH 3.4 with 5M KOH) in 250 mL shake-flasks at 30°C and 200 rpm in an orbital shaker. Carbon sources included 0, 10, or 100 g/L glucose along with 0 or 1 g/L 3HP. Samples were collected for RNA-seq analysis at 6 h and 18 h post-inoculation. RNAs from *A. pseduoterreus* samples were extracted from samples using a Maxwell-16 LEV Plant RNA kit (Promega, Madison, WI) and sequenced on an Illumina platform. Sequencing reads were mapped to *A. pseudoterreus* ATCC 32359 transcripts (Pomraning et al., 2022) and significantly differentially expressed genes determined using DESeq2(Love et al., 2014). The whole dataset is provided in Additional File 2.

2.10 qRT-PCR analysis of g2945

To compare relative mRNA expression levels of g2945, G-g2945, T-g2945 and the control strain $MCR_{Ca\text{-}Split}$, were cultured in SD medium and 12 OD_{600} unit samples were taken on day 1 and 3. Harvested cell pellets were frozen immediately in liquid nitrogen and total RNAs were extracted using RNeasy Mini Kit (Qiagen). Concentration of isolated total RNA were measured by NanoDrop® ND-1000 UV-Vis Spectrophotometer (Thermo Scientific). Quantitative reverse transcription PCR (qRT-PCR) was performed using Luna® Universal One-Step RT-qPCR Kit (New England BioLabs). Endogenous ACTIN (RTO4_14107) was used as a reference gene and $MCR_{Ca\text{-}Split}$ was as a negative control strain. ACTIN was detected by ACTIN forward (5'-gtcttcccctcgattgtcgg-3') and reverse (5'-tcgatggggtacttgagggt-3') primers. For detecting N-terminal part of g2945, g2945-qPCR-primer2 forward (5'-cttctccctctccctccctc-3') and reverse (5'-gctggtagaccgagaacgag-3') primers were used. For confirming C-terminal part of g2945, g2945-qPCR-primer5 forward (5'-cgctcctcatctactgctgg-3') and reverse (5'-ggtgcccgtcttcttgatgt-3') primers were used. All primers for qRT-PCR were designed by NCBI primer-BLAST

(https://www.ncbi.nlm.nih.gov/tools/primer-blast/). All experiments were performed in three biological and three technical replicates.

Results

3.1 Construction of 3HP biosynthesis pathway in R. toruloides

We decided to focus on the malonyl-CoA to 3HP pathway because *R. toruloides* is oleaginous and therefore naturally has a high flux towards malonyl-CoA(Lee et al., 2022). We codon optimized and expressed the malonyl-CoA reductase from *C. aurantiacus* (MCR_{Ca}) using two approaches. First, MCR_{Ca} was expressed intact under control of the forward orientation of a strong, constitutive, and bi-directional promoter previously characterized by Nora et al(Nora et al., 2019). Second, to balance the enzyme activities of MCR_{Ca}, we also split the MCR_{Ca} gene encoding the N-terminal and C-terminal portions of the protein ($MCR_{Ca\text{-}Split}$) and expressed them separately under both orientations of this promoter(Liu et al., 2016) (Fig. 1).

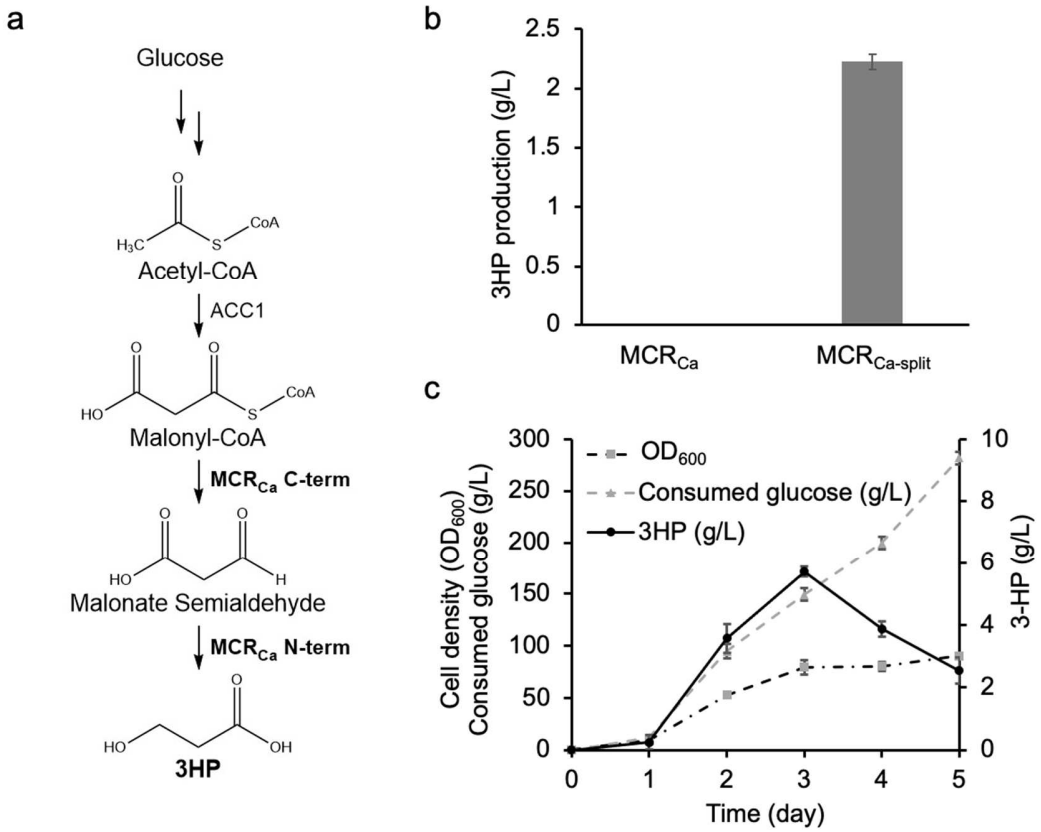

Fig. 1. Schematic and results of 3HP production via the malonyl-CoA pathway in *R. toruloides*. (a) The reactions performed by the bifunctional enzyme, malonyl-CoA reductase from *C. aurantiacus* (MCR_{Ca}), are split into the N- and C-terminal components. (b) 3HP production from malonyl-CoA pathway in test tubes cultured in SD medium. All error bars represent standard deviations of biological triplicates. MCR, malonyl-CoA reductase. MCR-split, malonyl-CoA reductase with split C- and N- termini. (c) 3HP production in Ambr® 250 bioreactor cultured in YP20D media. Error bars represent standard deviation from triplicate runs.

We integrated these cassettes into the *CAR2* locus of *R. toruloides* for the robustness of integration and ease of screening at this locus and cultured the strains in SD medium (10% glucose) for three days in test tubes. Extracellular supernatant was then collected and analyzed

via HPLC to screen for 3HP production. The strain harboring the $MCR_{Ca\text{-}Split}$ gene produced 2.2 ± 0.1 g/L 3HP, while that harboring the intact MCR_{Ca} gene failed to yield any measurable 3HP (Fig. 1b). The results, together with others' observations(Liu et al., 2016), collectively indicate the importance of individually expressing and balancing the two functional domains of MCR_{Ca}.

We dubbed the strain successfully producing 3HP "$MCR_{Ca\text{-}Split}$". To test the scalability of this process, we followed up by performing an Ambr® 250 run. After 5 days of cultivation, the culture reached an OD_{600} of 90.3 and 3HP production peaked on the 3rd day at 5.7 g/L, corresponding to a yield of 0.04 g 3HP/g glucose (Fig. 1c). The majority of cell growth happened on the first three days, reaching 88.3% of its maximum. Although cell growth and 3HP production dramatically slowed down or dropped after day 3, glucose consumption continued to steadily increase, which might be attributed to providing the maintenance energy of the cells. We observed a significant drop in 3HP titer from day 4, indicating *R. toruloides* can efficiently catabolize 3HP and may be stuck in a futile cycle of 3HP production and catabolism.

3.2 Addressing 3HP catabolism in R. toruloides

To confirm 3HP could be consumed, we grew WT *R. toruloides* in minimal media spiked with 8 g/L 3HP. Over the course of three days, we observed no reduction in 3HP in blank media (9.3 ± 1.7 g/L) (Fig. 2a). However, media inoculated with *R. toruloides* had only 1.6 ± 0.1 g/L 3HP, significantly lower than the blank media (P = 0.02). This shows that *R. toruloides* is capable of catabolizing 3HP.

To better understand the consumption of 3HP by *R. toruloides*, we performed RB-TDNA sequencing of *R. toruloides* grown with 3HP or various other carbon sources. We employed a

pooled library of *R. toruloides* variants with barcoded sequences randomly integrated into the genome(Coradetti et al., 2018), grown for 3 days. Barcodes which were significantly underrepresented during growth on a particular carbon source are indicative of the genetic loci of potential genes associated with consumption of that carbon source. We selected the top 100 genes that showed fitness defects in 3HP, out of which 30 genes were directly involved in metabolic pathways and were ranked based on their fitness defects in 3HP (Fig. 2b). Among these 30 genes, about half of the genes also exhibit significant fitness defects in propionate, butyrate and 3-hydroxybutyrate, which suggest that these genes are likely involved in general short chain acid metabolism and not specific for 3HP. We also observed a correlation between these fitness values and those obtained during growth on either valine or leucine as the primary carbon source (Supplementary Fig. 1), indicative of a potential link between catabolism of 3HP and branched chain amino acid metabolism in *R. toruloides.* This link between 3HP and branched-chain amino acid catabolism has also been previously reported in *Cupriavidus necator*(Arenas-López et al., 2019).

One of the genes identified in this library, *RTO4_8975*, was notable. We have previously reported that deletion of the putative malonate semialdehyde dehydrogenase gene, Ap*ald6*, abated 3HP consumption by the fungus *A. pseudoterreus*(Pomraning et al., 2021). The protein encoded by *RTO4_8975* shares 56% protein sequence homology with this gene. We therefore sought to delete *RTO4_8975* by employing our recently developed CRISPR-Cas system(Otoupal et al., 2019). Sanger sequencing confirmed a 13 bp indel near the cut site, causing a frame-shift and effectively eliminating the expression of this gene (Supplementary Fig. 2). This deletion caused no impact on growth in a mixed glucose-3HP minimal media (Fig. 2c). However, with

3HP as the sole carbon source, growth was significantly hindered (P = 0.006) relative to WT *R. toruloides* (Fig. 2c). Additionally, significantly (P = 0.04) greater 3HP remained after cultivation in the WT Δ*RTO4_8975* strain (Fig. 2d). This further confirms the role of this putative malonate semialdehyde dehydrogenase in catabolism of 3HP. We therefore chose to refer to *RTO4_8975* hereafter as *ALD6*.

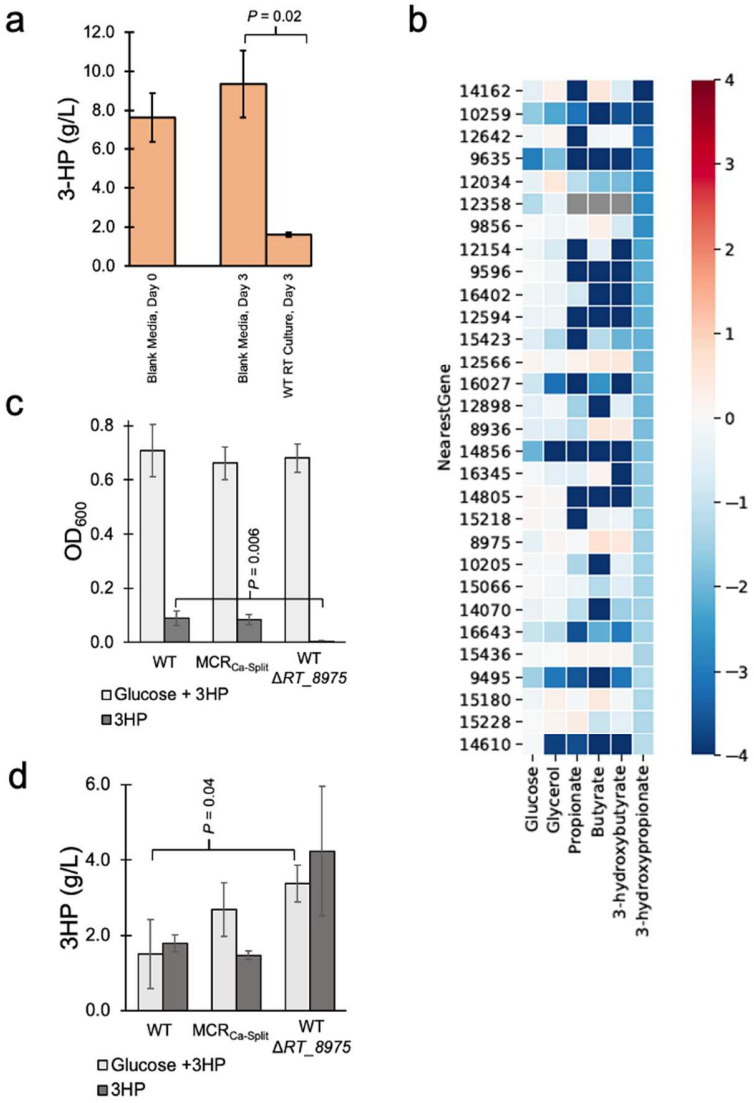

Fig 2. Identification and deletion of genes involved in 3HP catabolism. The *R. toruloides* gene *RTO4_8975*, annotated as an aldehyde dehydrogenase, was identified from RB-TDNAseq and deleted in the WT using CRISPR-Cas9, and compared against WT and $MCR_{Ca\text{-}Split}$ strains

for its ability to consume 3HP in minimal media. (a) Cell growth of WT in minimal media supplemented with 3HP as the sole carbon source. (b) Fitness scores of potential genes involved in 3HP catabolism. Fitness scores were obtained in several carbon sources, including 3HP and a number of reference carbon sources. The top 100 genes that exhibit most significant fitness defects in 3HP were selected, out of which genes directly associated with metabolic enzymatic reactions were ranked based on their fitness defects in 3HP and plotted. (c) Growth of WT, $MCR_{Ca\text{-}Split}$, and WT with *RTO4_8975* deleted in minimal media supplemented with glucose and 3HP, or 3HP as the sole carbon source were measured. (d) Titers of remaining (or produced) 3HP in minimal media cultures. All error bars represent standard deviations of triplicates. All *P*-values were calculated using a two-tailed type II Student's *t*-test.

3.3 Engineering 3HP transporter in R. toruloides

Once we were able to prevent 3HP consumption by deleting catabolic genes, we shifted our attention to improving production of 3HP by enhancing its export outside of the cell. Our metabolomic analysis of $MCR_{Ca\text{-}Split}$ indicates that there was intracellular accumulation of 3HP (Supplementary Fig. 3, Additional File 3). This suggests that engineering enhanced 3HP transport to facilitate the export of 3HP from the cell may improve 3HP titers. To the best of our knowledge there are no 3HP transporters in eukaryotes reported in the literature. Previously reported 3HP transporter YohJK was found to improve 3HP titers in *K. pneumoniae* and *E. coli*(Nguyen-Vo et al., 2022, 2020), however no close homology of this protein was found in *R. toruloides*. A few transporters have been characterized and reported in the literature for monocarboxylic acids with similar chemical structures to 3HP, such as lactic acid and propionic acid(Casal et al., 2008; Sá-Pessoa et al., 2013; Vieira et al., 2010). These transporters have been found to show broad substrate specificities, thus making them potential transporter candidates for

3HP. Here we expressed two *R. toruloides* monocarboxylic acid transporters that are homologous to two characterized lactic acid transporters in *S. cerevisiae*, Ady2 (RTO4_10658) and JEN1 (RTO4_10184) under the control of a pTEF1 and pPKG1 promoter, respectively.

In addition to targeting transporters based on molecular overlap, we identified and expressed a candidate 3HP transporter from *A. pseudoterreus*. *A. pseudoterreus* is known to have high acid tolerance and has been widely engineered to produce various organic acids, therefore we hypothesized organic acid transporters likely exist in this organism. Previously three 3HP producing strains, 3HP+, *cad*::3HP+ and *cad*::3HP+, 3HP+, were constructed in a study by Pomraning *et al*. These three strains express one or two copies of a 3HP biosynthetic pathway in in the *A. pseudoterreus* genome with and without knocking out the gene *cad1* that encodes cis-aconitate decarboxylase (Pomraning et al., 2021). Global proteomics data from *A. pseudoterreus* strains that produce 3HP was compared with non-producer strains(Pomraning et al., 2021) to identify transporters that are upregulated in producer strains. In addition, we performed transcriptomic analysis to compare changes in transcript levels from a non-producer strain growing with 3HP as the sole carbon source or with 3HP spiked into production medium against unspiked controls to identify 3HP responsive genes (Fig. 3). From this analysis, g2945 (jgi|Asppseute1|473891) was identified as a 3HP responsive MFS monocarboxylate transporter that may be involved in 3HP transport across the plasma membrane of *A. pseudoterreus*. Notably, this transporter is upregulated in strains that accumulate 3HP intracellularly as well as in conditions where extracellular 3HP is metabolized, suggesting transport may be bidirectional and dependent on the concentration gradient of 3HP and any coupling ions involved.

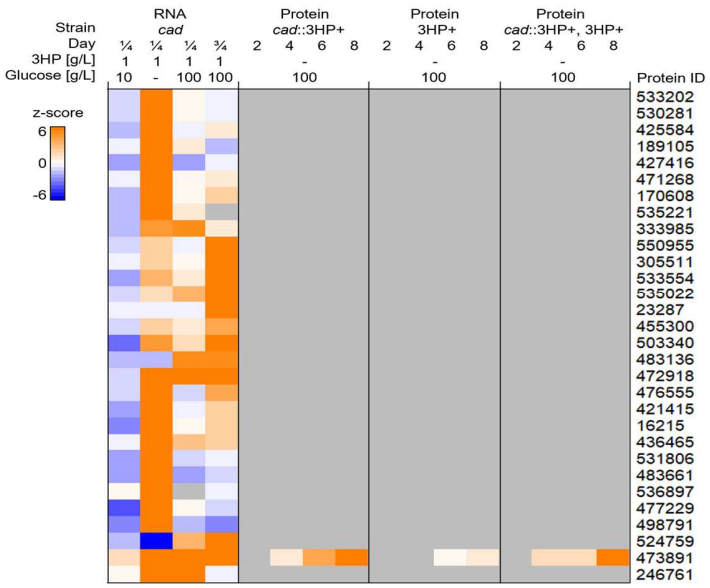

Fig 3. 3HP responsive MFS transporters in *Aspergillus pseudoterreus*. A non-3HP producing *A. pseudoterreus* strain was examined by RNA-seq for genes that increase in expression level in response to spiked 3HP present as a sole carbon source or in production conditions. Z-scores indicate change versus conditions without spiked 3HP. 3HP producing *A. pseudoterreus* strains were examined by proteomics for genes that increase in expression level in response to the presence of the 3HP production pathway. Z-scores indicate change versus unengineered parental strains. The 30 MFS transporters with the highest average increase in expression level across the datasets are shown. The MFS transporter g2945 (jgi|Asppseute1|473891) was chosen for overexpression. *cad*::3HP+, 3HP+ and *cad*::3HP+, 3HP+ are three previously developed 3HP producing *A. pseudoterreus* strains(Pomraning et al., 2021).

We codon optimized the transporter g2945 under the control of two commonly used *R. toruloides* promoters, pGAPDH and pTEF1, and expressed it at the *Ku70* locus in the $MCR_{Ca\text{-}Split}$ strain. After 3 days of cultivation in SD medium, the Ady2 and JEN1 overexpression strains did not exhibit any changes in 3HP titers compared to the parent strain whereas a significant increase

in 3HP production was observed with g2945 overexpression (Fig. 4). Compared to the parent $MCR_{Ca\text{-}Split}$ strain that produces 2.0 ± 0.08 g/L 3HP, the g2945 overexpression strain yielded 5.4 ± 0.16 g/L and 9.2 ± 0.08 g/L 3HP with the pGAPDH and pTEF1 promoters (strains denoted as G-g2945 and T-g2945), respectively. This supports our hypothesis that 3HP export may be limiting the 3HP production in the $MCR_{Ca\text{-}Split}$ strain. Engineering enhanced 3HP export may enhance 3HP titers by improving the thermodynamic favorability of the pathway and reducing the opportunity for intracellular 3HP to be catabolized. In addition, our previous transcriptomic and GFP expression results suggest that pTEF1 is a stronger promoter than pGAPDH(Nora et al., 2019), which indicates the higher production of 3HP with TEF1 promoter is likely correlated with increased transporter expression. We further performed qRT-PCR to quantify the relative mRNA levels of the g2945 transporter in these two strains and the results confirmed higher transcript levels in the T-g2945 strain (Supplementary Fig. 4).

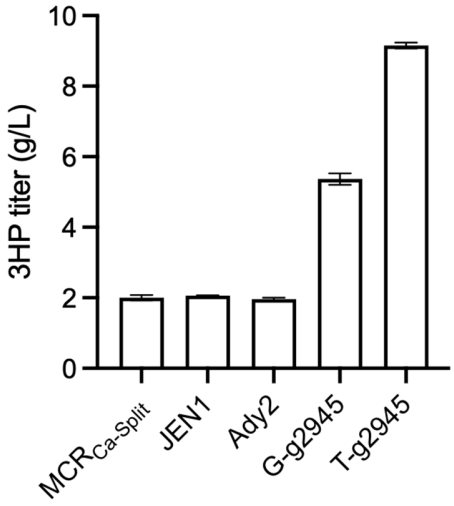

Fig 4. 3HP transporter engineering in *R. toruloides*. Two *R. toruloides* transporters homologous to reported monocarboxylic acid transporters in *S. cerevisiae*, JEN1 and Ady2, were overexpressed in $MCR_{Ca\text{-}Split}$. In addition, a predicted 3HP transporter in *A. pseudoterrus*, g2945,

was expressed under the pGAPDH and pTEF1 promoters in $MCR_{Ca\text{-}Split}$. Error bars represent standard deviation of biological triplicates.

3.4 Medium optimization to enhance 3HP production in R. toruloides

Alongside genetic engineering approaches, process optimization has shown to be important in optimization of bioproduct titers, rates and yields in *R. toruloides*. As it is technoeconomically and environmentally favorable to produce bioproducts from lignocellulosic hydrolysate, here we focus on media optimization of a hydrolysate developed by deacetylation and mechanical refining (DMR) (Chen et al., 2016) processing of corn stover biomass (denoted as DMR hydrolysate) and a SD mock hydrolysate that contains similar levels of glucose and xylose (denoted as mock hydrolysate). It has been well established that different nitrogen sources and C:N ratios lead to significant global metabolic shifts in *R. toruloides*, which can lead to very different flux towards bioproducts(Wehrs et al., 2019; Ye et al., 2021).

Here we used the $MCR_{Ca\text{-}Split}$ strain and focused on two different nitrogen sources, ammonium sulfate and urea, and varied the C:N ratios at 4, 8, 40, and 160. In the mock hydrolysate medium (Fig. 5a), an increase in 3HP titers was observed with increase in C:N ratios in both nitrogen sources. The highest 3HP titer reached 7.3 g/L with urea as the nitrogen source at a C:N ratio of 40. In the DMR hydrolysate medium, compared to ammonium sulfate, urea conditions exhibited significantly higher 3HP titers at all C:N ratios tested (Fig. 5b). At an 8:1 C:N ratio, the 3HP titer reached 10.7 g/L, which represents a 4.8-fold increase from our initial medium condition. Cell growth measurement at OD_{600} showed similar biomass accumulation in urea at C:N ratio 4:1 and 8:1 compared to other nitrogen conditions in DMR medium (Supplementary Fig. 5), which indicates the differences in 3HP titers we observed are not caused by differences in cell growth.

Interestingly, we observed significant drops in pH for most of the ammonium sulfate conditions to as low as pH 2.0 (Supplementary Fig. 5), whereas most of the urea conditions stayed at higher pH (between pH 5.0 - 9.0). The higher pH under urea conditions is likely caused by the assimilation of urea by urease, where two NH_3 molecules are released and thus increasing the pH. Based on these results, we selected the DMR hydrolysate with urea and 8:1 C:N ratio (denoted as DMR8U media) for our further strain engineering efforts.

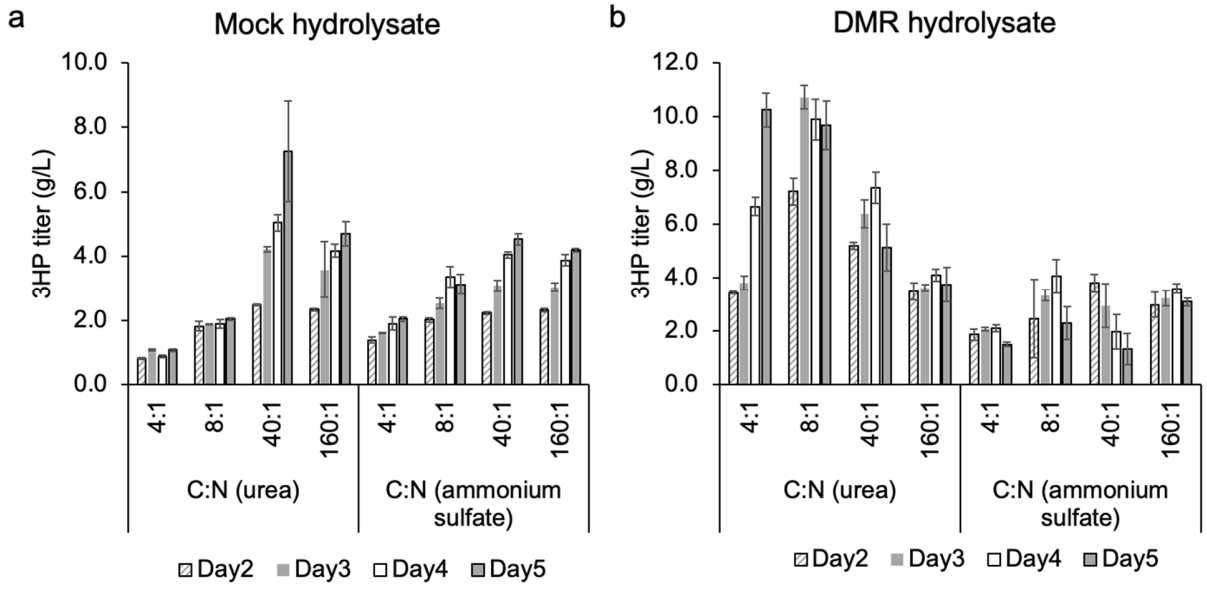

Figure 5. Media optimization to enhance 3HP titers in the $MCR_{Ca\text{-}Split}$ strain. Two nitrogen sources, urea and ammonium sulfate, were tested and varied at various C:N ratios in the mock hydrolysate media and DMR hydrolysate media.

To gain insights into the metabolic shifts that may lead to increased 3HP production, we performed global proteomic and metabolomic analysis of $MCR_{Ca\text{-}Split}$ in DMR hydrolysate containing urea and ammonium sulfate at two drastically different C:N ratios, 4:1 and 160:1 (Additional File 4 and Additional File 5). We selected two time points, day 3 and day 5, to

represent an early and a late stage in 3HP fermentation. We observed drastically different expressions of proteins involved in nitrogen metabolism (Fig. 6, Additional File 4). The expression of arginase, asparagine synthase and glutamate dehydrogenase (NAD-dependent, involved in glutamate degradation) were upregulated in urea media with 4:1 C:N ratio (denoted as DMR4U), whereas glutamine synthetase and glutamate dehydrogenase (NADP-dependent, involved in glutamate biosynthesis) levels were downregulated in both nitrogen sources with 4:1 C:N ratio. Previous studies have shown that in *R. toruloides* uptake of urea is markedly faster than that of $NH4^+$ and intracellular $NH4^+$ can be rapidly released(EVANS and RATLEDGE, 1984), which may have contributed to activation of the nitrogen catabolic enzymes under high urea conditions and accumulation of nitrogen containing metabolites in these pathways (Fig. 6). The down-regulation of glutamine synthetase under high nitrogen conditions indicates potential repression of these proteins by $NH4^+$.

In addition, we also observed elevated levels of acetyl-CoA carboxylase in DMR4U media, which have shown to be key to enhancing the precursor of 3HP, malonyl-CoA, in various hosts. Meanwhile, ATP citrate lyase and carnitine o-acetyltransferase levels were both upregulated in DMR4U, which may further contribute to elevated acetyl-CoA levels. It was also interesting to find that the MCR expression levels were slightly higher in DMR4U, which may have also contributed to the enhanced 3HP production under this condition. The expression of ALD6 was also slightly elevated in DMR4U, suggesting potentially more active 3HP catabolism and further motivating knocking out this gene to enhance 3HP production.

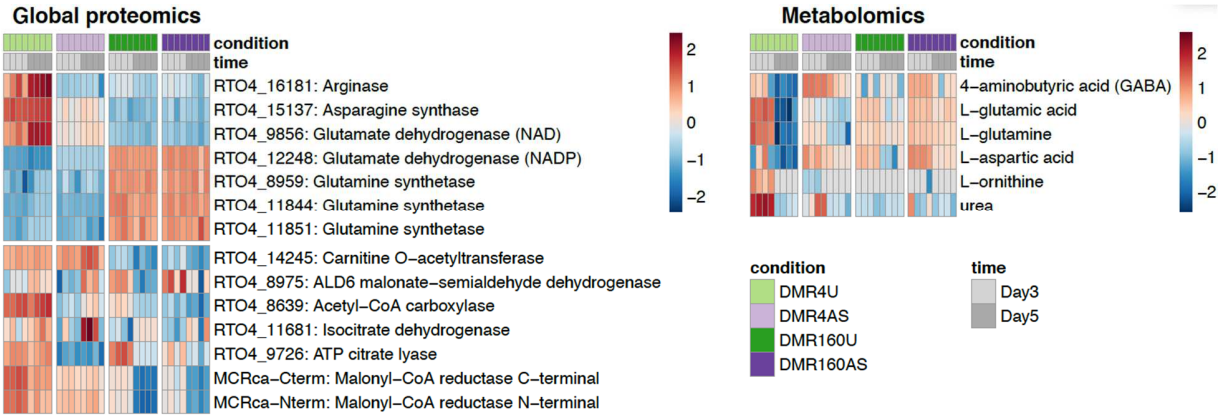

Figure 6. Global proteomic and metabolomic analysis to elucidate shifts in nitrogen metabolism and 3HP pathways in two nitrogen sources, urea and ammonium sulfate. Proteins and metabolites involved in nitrogen metabolism and pathways relevant to 3HP accumulation were plotted. Colors indicate row-wise scaled log2 abundance. DMR4U, DMR media with urea at 4:1 C:N ratio. DMR4AS, DMR media with ammonium sulfate at 4:1 C:N ratio. DMR160U, DMR media with urea at 160:1 C:N ratio. DMR160AS, DMR media with ammonium sulfate at 160:1 C:N ratio.

3.5 Combinatorial strain engineering to address 3HP transport and catabolism

As we identified two pathway modifications that improve 3HP titers, a rational next step is to stack these modifications to further improve titers, rates and yields. To this end, we took the $MCR_{Ca\text{-}Split}$ strain with the transporter overexpression under the control of TEF1 promoter (T-g2945 strain) and deleted *ALD6* by homologous recombination (strain denoted as ALD6-g2945). To enhance the carbon flux from malonyl-CoA to 3HP, we also expressed a second copy of $MCR_{Ca\text{-}Split}$ at the *ALD6* locus (strain denoted as MCR-ALD6-g2945). These strains were cultured in parallel with the parent strains in a 48-well FlowerPlate in the optimized media conditions as discussed above (DMR8U media).

In the $MCR_{Ca\text{-}Split}$ strain, 3HP titer peaked at 3 days reaching 9.8 g/L and then dropped (Fig. 7a). The drop is likely due to the active catabolic activities toward 3HP in this strain. Compared to $MCR_{Ca\text{-}Split}$, the T-g2945 strain titer increased by 48.0%, reaching 14.5 g/L 3HP at day 6. Although T-g2945 strain has the 3HP catabolic pathway intact, the transporter actively exports 3HP to the media, thus alleviating the degradation of 3HP. Both ALD6-g2945 and MCR-ALD6-g2945 strains exhibited improved titers compared to the parent T-g2945 strain, reaching 18.7 g/L and 19.2 g/L respectively. ALD6-g2945 and MCR-ALD6-g2945 strains showed slightly faster glucose utilization for the first two days, and almost all the glucose was consumed for all the strains after 3 days (Fig. 7b). Xylose utilization started between day 2 and day 3 when glucose levels dropped to close to zero, and the xylose utilization rates did not show any significant differences among the four strains (Fig. 7c). We found that the additional copy of MCR in the MCR-ALD6-g2945 strain did not have any significant impact on 3HP production, indicating that the supply of upstream precursors, i.e. malonyl-CoA, is likely a rate-limiting factor in these strains. Thus, further engineering strategies designed to enhance the pool of precursors in these strains will likely be fruitful.

In addition, we further evaluated the stability of the MCR-ALD6-g2945 strain both at the ensemble level and the individual cell level (see Materials and Methods for details). Our results showed no significant differences in 3HP production over the passages, suggesting the strain being genetically stable, at least within the time tested (Supplementary Fig. 6).

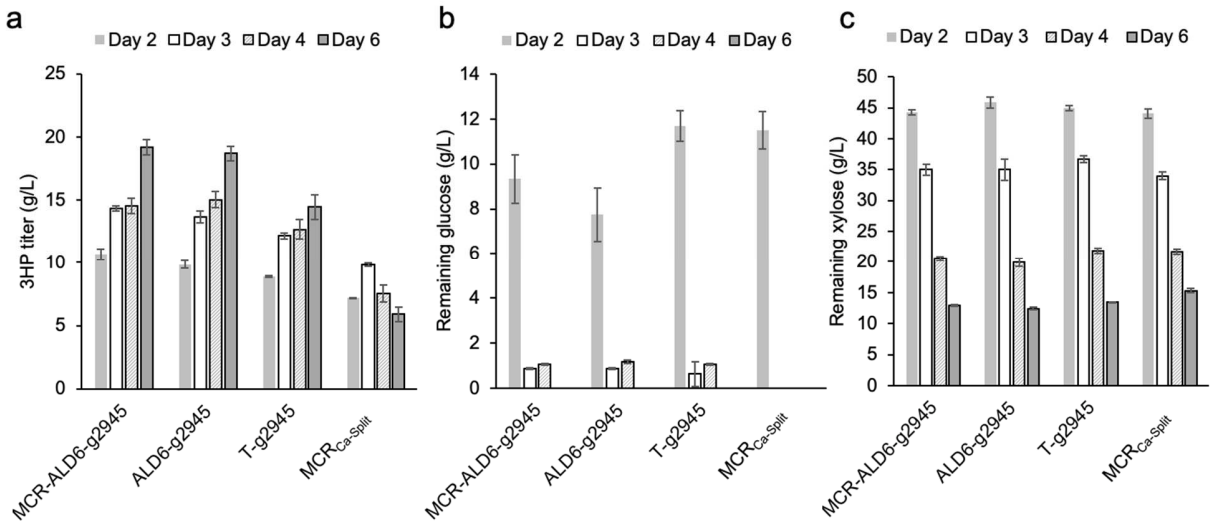

Figure 7. Production of 3HP and sugar utilization in engineered *R. toruloides* strains. Strains were cultivated in the DMR8U media for 6 days. g2945, g2945 transporter expression under TEF1 promoter in $MCR_{Ca\text{-}Split}$. ALD6-g2945, *ALD6* knockout in g2945 strain. MCR-ALD6-g2945, ALD6-g2945 strain with a second copy of $MCR_{Ca\text{-}Split}$ expressed at the *ALD6* locus. Error bars represent standard deviations of biological triplicates.

3.6 Bioreactor scale-up of the combinatorial strain

Following strain and cultivation condition optimization, we then sought to further enhance 3HP production and demonstrate the feasibility of process scale-up in a 2-L fed-batch bioreactor. The modified DMR8U media (see methods) was used during the batch fermentation, and glucose was fed manually when glucose level dropped below 20 g/L. The maximum cell growth and 3HP production were obtained at 102 hrs, reaching an OD_{600} of 155.2 and 45.4 g/L respectively (Fig. 8a). In the first 79 hrs, the strain grew rapidly and reached 86.3% of the maximum cell density. Consistent with what we observed at the bench-scale, the strain consumed glucose and xylose simultaneously, where the initial glucose was depleted after 22 hrs of cultivation and initial

xylose was depleted after 48 hrs. In addition, we also observed short periods of reduced cell growth rates and 3HP production (31 hrs, 55 hrs and 96 hrs) during the course of the fermentation, which are likely caused by the low sugar levels at those time points. This suggests further process optimization to maintain higher glucose levels could potentially increase the rates of 3HP production. We obtained a maximum 3HP productivity and yield of 0.44 g/L/h and 0.11 g/g sugars at 102 hrs. Although ALD6 was knocked out to turn down 3HP catabolism, we still observed a drop in 3HP titer towards the end of the fermentation. This might indicate activation of an alternative 3HP catabolic pathway (such as the reductive pathway, as described in Supplementary Fig. 7) at late growth phase.

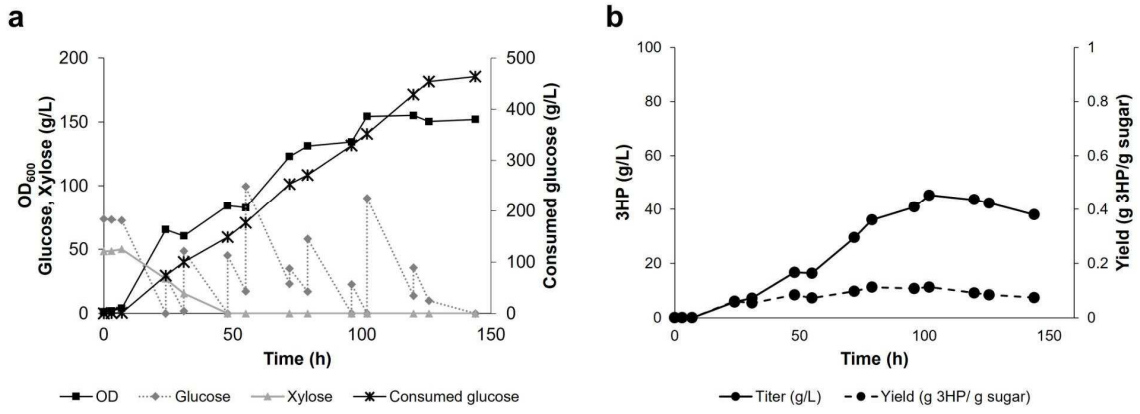

Fig 8. Fed-batch fermentation of MCR-ALD6-g2945 strain for 3HP production in a 2 L bioreactor. (A) Cell growth, residual concentration of glucose and xylose, and consumed glucose concentrations. (B) 3HP titer and yield.

Discussion

Microbial production of value-added bioproducts is an attractive alternative to the current chemical industry. To make these technologies economically viable, it is key to improve titers,

rates and yields. Furthermore, to make this production both economically and environmentally sustainable, it must be based on renewable feedstocks such as deconstructed lignocellulosic hydrolysate. Here we engineer the oleaginous yeast *R. toruloides* to valorize low-cost biomass into 3HP through the malonyl-CoA route. Pathway optimizations to reduce 3HP catabolism and promote 3HP export were then introduced and led to significantly enhanced 3HP production. We obtained a titer of 45.4 g/L in a 2-L bioreactor from a corn stover hydrolysate supplemented with glucose feeding with minimal addition of nutrients. The glucose feeding is not ideal for an industrial process but indicates that strain has capacity for conversion of hydrolysates with higher sugar concentrations if they were to be developed. Further work needs to be done to optimize this strain and conversion process to improve efficiency, but our work suggests there is potential for additional improvements beyond what we have accomplished with the mixed feed process.

1) Alternative pathways for 3HP catabolism

We discovered early in this work that *R. toruloides* has the capacity to consume 3HP in the absence of glucose. Previous studies have proposed two potential routes for 3HP degradation, including a reductive pathway and an oxidative pathway(Yang et al., 2017b). The reductive pathway converts 3HP to propionyl-CoA, which then enters the TCA cycle through the 2-methylcitrate cycle (Supplementary Fig. 7). The oxidative pathway involves a one-step conversion of 3HP into malonate semialdehyde (3OP), which will be then converted to acetyl-CoA through 3OP dehydrogenase. To elucidate which pathway *R. toruloides* employs to consume 3HP, we performed an RB-TDNA Seq experiment(Coradetti et al., 2018). Our results suggested correlation between the 3HP degradation with the branched chain amino acid (valine

and leucine) pathway in *R. toruloides*, which corresponds to the reductive degradation pathway that produces propionyl-CoA (Supplementary Fig. 7). Indeed, a number of genes involved in the valine pathway were ranked among the top 30 genes that showed most significant fitness defects in 3HP (Fig. 2b). A biosensor designed based upon a 3HP-responsive transcription factor was found to also be induced in the presence of valine, highlighting the possible connection between valine and 3HP consumption(Nguyen et al., 2019). Furthermore, we also observed increased heptadecanoic acid levels through our metabolomic analysis (Supplementary Fig. 7), which could be caused by a higher level of 3HP-derived propionyl-CoA. We found that deleting the oxidative degradation pathway by deleting *ALD6* eliminated a large portion of 3HP catabolism, which indicates this pathway accounts for the majority of the 3HP catabolic activity in this host, as has been observed in other hosts(Pomraning et al., 2021; Zhou et al., 2014, 2013). However, it is possible that the 3HP reductive degradation pathway may be active under certain conditions, which may explain the 3HP degradation we observed in the late growth stage during our bioreactor fermentation. To further reduce 3HP catabolism, disrupting the 3HP reductive degradation pathway may be fruitful. However, caution should be taken as the pathway likely overlaps with the native branched-chain amino acid pathway.

2) Effects of nitrogen sources on 3HP production

It has been well recognized that process optimization of cultivation conditions is valuable to improve bioproduct titers, rates and yields. Previous studies in *R. toruloides* have found that the nitrogen source and C:N ratios have significant impacts on various bioproducts(LI et al., 2006). Here we found the use of urea as the nitrogen source significantly enhanced 3HP production compared to ammonium sulfate, which is consistent with a previous study that engineered *R.*

toruloides to produce indigoidine(Wehrs et al., 2019). These findings are in agreement with a previous study(EVANS and RATLEDGE, 1984) that reports a faster urea uptake than $NH4^+$, partly due to increased urease activity when urea is used as the nitrogen source. Consistent with a previous study, we found that a C:N ratio of 8:1 in DMR hydrolysate media containing urea yielded the highest 3HP production after 3 days(Wehrs et al., 2019). A deviation from this ratio (C:N ratio of 4 or 40) led to lower titers. The C:N ratio of 4:1 led to comparable final titers at day 5 in DMR hydrolysate media. However, the productivity was significantly lower in the first 4 days. In most of the conditions employing ammonium sulfate media the pH dropped below the pKa of 3HP (pKa = 4.5), meaning that 3HP was in the acidic form. By comparison, the pH of most of the conditions employing urea media stayed above the pKa, and thus 3HP was in the charged form. As it is generally regarded that monocarboxylic acid transport happens in the neutral form across cell membranes(Casal et al., 2008), the higher pH in the urea media may hinder the re-uptake of 3HP and contribute to enhanced 3HP titers. In addition, our global proteomic and metabolomic analysis also found enhanced nitrogen metabolism and increases in levels of proteins that are involved in the synthesis of 3HP in optimized media conditions. These likely have contributed to the significant increase in 3HP titers in DMR urea media.

3) Potential engineering strategies to further improve 3HP production

As an oleaginous organism, *R. toruloides* is known to exhibit high flux towards the precursors of lipids, malonyl-CoA(Zhang et al., 2016, 2021). Therefore, we anticipated that the upstream metabolic flux was not the major factor limiting our 3HP titers. Due to the abundance of malonyl-CoA in *R. toruloides*, we instead focused on optimizing the downstream pathways by alleviating the product catabolism and promoting its export. However, in our final engineered

strain (MCR-ALD6-g2945), the synthesis of malonyl-CoA appears to be a rate-limiting step, as no increase in 3HP is observed with an additional copy of MCR. Malonyl-CoA is synthesized from acetyl-CoA by acetyl-CoA carboxylase (Acc). Previously, the overexpression of Acc has been found to enhance lipid production in this and other hosts(Liu et al., 2015; Runguphan and Keasling, 2014; Zhang et al., 2016), and may thus be a promising next step to further enhance titers. In addition, further engineering strategies to enhance the pool of upstream precursors, acetyl-CoA, may lead to additional improvement in 3HP titers as has been shown in malonyl-CoA derived bioproducts from other oleaginous species(Qiao et al., 2015; Wang et al., 2020). Furthermore, we observed significant accumulation of biomass during the fermentation, which suggests room to enhance 3HP yields by reducing carbon flux towards biomass. Finally, as *R. toruloides* is known to naturally divert a large pool of malonyl-CoA and its upstream metabolite acetyl-CoA towards the synthesis of carotenoids and lipids(Zhu et al., 2012), it may also be beneficial to reduce expression of these pathways in future studies. These strategies can be potentially fruitful to divert more carbon flux towards 3HP to increase product titers, rates, and yields.

Conclusions

This study demonstrates the production of 3HP in *R. toruloides* for the first time. We leveraged the naturally high flux towards malonyl-CoA in this host and implemented functional genomics and bioinformatic analysis to identify potential genetic modifications to improve production. By reducing 3HP catabolism and promoting its export, we reached a titer of 45.4 g/L in a 2-L fed-batch bioreactor fermentation of deconstructed lignocellulosic hydrolysate and glucose feed. Further genetic engineering of the global metabolism to optimize the supply of key precursors,

such as acetyl-CoA and malonyl-CoA, as well as cofactors and bottleneck steps, and reducing carbon flux towards biomass accumulation will likely lead to further enhanced 3HP titers and yields. These results indicate that *R. toruloides* is an attractive host for malonyl-CoA derived bioproducts from cheap renewable carbon feedstocks.

Competing financial interests

The authors claim no competing financial interests.

Acknowledgement

Sandia National Laboratories is a multi-mission laboratory managed and operated by National Technology and Engineering Solutions of Sandia, LLC., a wholly owned subsidiary of Honeywell International, Inc., for the U.S. Department of Energy's National Nuclear Security Administration under contract DE-NA0003525. This research was part of the Agile BioFoundry (https://agilebiofoundry.org) supported by the U. S. Department of Energy, Energy Efficiency and Renewable Energy, Bioenergy Technologies Office, through contract DE-AC02-05CH11231 between Lawrence Berkeley National Laboratory and the U. S. Department of Energy. The work was supported by Agile BioFoundry (http://agilebiofoundry.org), funded by the United States Department of Energy, Office of Energy Efficiency and Renewable Energy, Bioenergy Technologies Office, under Award No. DE-NL0030038 for PNNL. A portion of this research was performed on a project award (10.46936/reso.proj.2020.51637/60000235) from the Environmental Molecular Sciences Laboratory, a DOE Office of Science User Facility sponsored by the Biological and Environmental Research program under Contract No. DE-AC05-

76RL01830. Pacific Northwest National Laboratory (PNNL) is operated for the U.S. Department of Energy by Battelle Memorial Institute under contract DE-AC05-76RL01830. The portion of the work conducted by the DOE Joint BioEnergy Institute (http://www.jbei.org) was supported by the US Department of Energy, Office of Science, Office of Biological and Environmental Research, through contract DE-AC0205CH11231 with Lawrence Berkeley National Laboratory. The views and opinions of the authors expressed herein do not necessarily state or reflect those of the United States Government or any agency thereof. Neither the United States Government nor any agency thereof, nor any of their employees, makes any warranty, expressed or implied, or assumes any legal liability or responsibility for the accuracy, completeness, or usefulness of any information, apparatus, product, or process disclosed, or represents that its use would not infringe privately owned rights. The Department of Energy will provide public access to these results of federally sponsored research in accordance with the DOE Public Access Plan (http://energy.gov/downloads/doe-public-access-plan).

References

Ageitos, J.M., Vallejo, J.A., Veiga-Crespo, P., Villa, T.G., 2011. Oily yeasts as oleaginous cell factories. Appl Microbiol Biotechnol 90, 1219–1227. https://doi.org/10.1007/s00253-011-3200-z

Arenas-López, C., Locker, J., Orol, D., Walter, F., Busche, T., Kalinowski, J., Minton, N.P., Kovács, K., Winzer, K., 2019. The genetic basis of 3-hydroxypropanoate metabolism in Cupriavidus necator H16. Biotechnol Biofuels 12, 150. https://doi.org/10.1186/s13068-019-1489-5

Beerthuis, R., Rothenberg, G., Shiju, N.R., 2015. Catalytic routes towards acrylic acid, adipic acid and ε-caprolactam starting from biorenewables. Green Chemistry 17, 1341–1361. https://doi.org/10.1039/C4GC02076F

Borodina, I., Kildegaard, K.R., Jensen, N.B., Blicher, T.H., Maury, J., Sherstyk, S., Schneider, K., Lamosa, P., Herrgård, M.J., Rosenstand, I., Öberg, F., Forster, J., Nielsen, J., 2015. Establishing a synthetic pathway for high-level production of 3-hydroxypropionic acid in Saccharomyces cerevisiae via β-alanine. Metab Eng 27, 57–64. https://doi.org/10.1016/j.ymben.2014.10.003

Casal, M., Paiva, S., Queirós, O., Soares-Silva, I., 2008. Transport of carboxylic acids in yeasts. FEMS Microbiol Rev 32, 974–994. https://doi.org/10.1111/j.1574-6976.2008.00128.x

Chen, X., Kuhn, E., Jennings, E.W., Nelson, R., Tao, L., Zhang, M., Tucker, M.P., 2016. DMR (deacetylation and mechanical refining) processing of corn stover achieves high monomeric sugar concentrations (230 g L^{-1}) during enzymatic hydrolysis and high ethanol concentrations (>10% v/v) during fermentation without hydrolysate purification or concentration. Energy Environ Sci 9, 1237–1245. https://doi.org/10.1039/C5EE03718B

Chen, Y., Bao, J., Kim, I.-K., Siewers, V., Nielsen, J., 2014. Coupled incremental precursor and co-factor supply improves 3-hydroxypropionic acid production in Saccharomyces cerevisiae. Metab Eng 22, 104–109. https://doi.org/10.1016/j.ymben.2014.01.005

Cheng, Z., Jiang, J., Wu, H., Li, Z., Ye, Q., 2016. Enhanced production of 3-hydroxypropionic acid from glucose via malonyl-CoA pathway by engineered Escherichia coli. Bioresour Technol 200, 897–904. https://doi.org/10.1016/j.biortech.2015.10.107

Coradetti, S., Pinel, D., Geiselman, G., Ito, M., Mondo, S., Reilly, M., Cheng, Y.-F., Bauer, S., Grigoriev, I., Gladden, J., Simmons, B., Brem, R., Arkin, A., Skerker, J., 2017. Functional genomics of lipid metabolism in the oleaginous yeast Rhodosporidium toruloides. bioRxiv.

Coradetti, S.T., Pinel, D., Geiselman, G.M., Ito, M., Mondo, S.J., Reilly, M.C., Cheng, Y.-F., Bauer, S., Grigoriev, I. v, Gladden, J.M., Simmons, B.A., Brem, R.B., Arkin, A.P., Skerker, J.M., 2018. Functional genomics of lipid metabolism in the oleaginous yeast Rhodosporidium toruloides. Elife 7. https://doi.org/10.7554/eLife.32110

Das, L., Geiselman, G.M., Rodriguez, A., Magurudeniya, H.D., Kirby, J., Simmons, B.A., Gladden, J.M., 2021. Seawater-based one-pot ionic liquid pretreatment of sorghum for jet fuel production. Bioresour Technol Rep 13, 100622. https://doi.org/10.1016/j.biteb.2020.100622

della Pina, C., Falletta, E., Rossi, M., 2011. A green approach to chemical building blocks. The case of 3-hydroxypropanoic acid. Green Chemistry 13, 1624. https://doi.org/10.1039/c1gc15052a

EVANS, C.T., RATLEDGE, C., 1984. Influence of Nitrogen Metabolism on Lipid Accumulation by Rhodosporidium toruloides CBS 14. Microbiology (N Y) 130, 1705–1710. https://doi.org/10.1099/00221287-130-7-1705

Fillet, S., Adrio, J.L., 2016. Microbial production of fatty alcohols. World J Microbiol Biotechnol 32, 152. https://doi.org/10.1007/s11274-016-2099-z

Geiselman, G.M., Kirby, J., Landera, A., Otoupal, P., Papa, G., Barcelos, C., Sundstrom, E.R., Das, L., Magurudeniya, H.D., Wehrs, M., Rodriguez, A., Simmons, B.A., Magnuson, J.K., Mukhopadhyay, A., Lee, T.S., George, A., Gladden, J.M., 2020a. Conversion of poplar biomass into high-energy density tricyclic sesquiterpene jet fuel blendstocks. Microb Cell Fact 19, 208. https://doi.org/10.1186/s12934-020-01456-4

Geiselman, G.M., Zhuang, X., Kirby, J., Tran-Gyamfi, M.B., Prahl, J.-P., Sundstrom, E.R., Gao, Y., Munoz Munoz, N., Nicora, C.D., Clay, D.M., Papa, G., Burnum-Johnson, K.E., Magnuson, J.K., Tanjore, D., Skerker, J.M., Gladden, J.M., 2020b. Production of ent-kaurene from lignocellulosic hydrolysate in Rhodosporidium toruloides. Microb Cell Fact 19, 24. https://doi.org/10.1186/s12934-020-1293-8

Geiselman, G.M., Zhuang, X., Kirby, J., Tran-Gyamfi, M.B., Prahl, J.-P., Sundstrom, E.R., Gao, Y., Munoz Munoz, N., Nicora, C.D., Clay, D.M., Papa, G., Burnum-Johnson, K.E., Magnuson, J.K., Tanjore, D., Skerker, J.M., Gladden, J.M., 2020c. Production of ent-kaurene from lignocellulosic hydrolysate in Rhodosporidium toruloides. Microb Cell Fact 19, 24. https://doi.org/10.1186/s12934-020-1293-8

Ham, T.S., Dmytriv, Z., Plahar, H., Chen, J., Hillson, N.J., Keasling, J.D., 2012. Design, implementation and practice of JBEI-ICE: an open source biological part registry platform and tools. Nucleic Acids Res 40, e141–e141. https://doi.org/10.1093/nar/gks531

Hu, C., Zhao, X., Zhao, J., Wu, S., Zhao, Z.K., 2009. Effects of biomass hydrolysis by-products on oleaginous yeast Rhodosporidium toruloides. Bioresour Technol 100, 4843–4847. https://doi.org/10.1016/j.biortech.2009.04.041

Hügler, M., Menendez, C., Schägger, H., Fuchs, G., 2002. Malonyl-Coenzyme A Reductase from *Chloroflexus aurantiacus* , a Key Enzyme of the 3-Hydroxypropionate Cycle for Autotrophic CO_2 Fixation. J Bacteriol 184, 2404–2410. https://doi.org/10.1128/JB.184.9.2404-2410.2002

Ji, R.-Y., Ding, Y., Shi, T.-Q., Lin, L., Huang, H., Gao, Z., Ji, X.-J., 2018. Metabolic Engineering of Yeast for the Production of 3-Hydroxypropionic Acid. Front Microbiol 9. https://doi.org/10.3389/fmicb.2018.02185

Jiang, J., Huang, B., Wu, H., Li, Z., Ye, Q., 2018. Efficient 3-hydroxypropionic acid production from glycerol by metabolically engineered Klebsiella pneumoniae. Bioresour Bioprocess 5, 34. https://doi.org/10.1186/s40643-018-0218-4

Jiao, X., Zhang, Y., Liu, X., Zhang, Q., Zhang, S., Zhao, Z.K., 2019. Developing a CRISPR/Cas9 System for Genome Editing in the Basidiomycetous Yeast *Rhodosporidium toruloides*. Biotechnol J 14, 1900036. https://doi.org/10.1002/biot.201900036

Kildegaard, K.R., Wang, Z., Chen, Y., Nielsen, J., Borodina, I., 2015. Production of 3-hydroxypropionic acid from glucose and xylose by metabolically engineered Saccharomyces cerevisiae. Metab Eng Commun 2, 132–136. https://doi.org/10.1016/j.meteno.2015.10.001

Kim, Jinho, Baidoo, E.E.K., Amer, B., Mukhopadhyay, A., Adams, P.D., Simmons, B.A., Lee, T.S., 2021. Engineering Saccharomyces cerevisiae for isoprenol production. Metab Eng 64, 154–166. https://doi.org/10.1016/j.ymben.2021.02.002

Kim, Joonhoon, Coradetti, S.T., Kim, Y.-M., Gao, Y., Yaegashi, J., Zucker, J.D., Munoz, N., Zink, E.M., Burnum-Johnson, K.E., Baker, S.E., Simmons, B.A., Skerker, J.M., Gladden, J.M., Magnuson, J.K., 2021. Multi-Omics Driven Metabolic Network Reconstruction and Analysis of Lignocellulosic Carbon Utilization in Rhodosporidium toruloides. Front Bioeng Biotechnol 8. https://doi.org/10.3389/fbioe.2020.612832

Kirby, J., Geiselman, G.M., Yaegashi, J., Kim, J., Zhuang, X., Tran-Gyamfi, M.B., Prahl, J.-P., Sundstrom, E.R., Gao, Y., Munoz, N., Burnum-Johnson, K.E., Benites, V.T., Baidoo, E.E.K., Fuhrmann, A., Seibel, K., Webb-Robertson, B.-J.M., Zucker, J., Nicora, C.D., Tanjore, D., Magnuson, J.K., Skerker, J.M., Gladden, J.M., 2021. Further engineering of R. toruloides for the production of terpenes from lignocellulosic biomass. Biotechnol Biofuels 14, 101. https://doi.org/10.1186/s13068-021-01950-w

Kumar, V., Ashok, S., Park, S., 2013. Recent advances in biological production of 3-hydroxypropionic acid. Biotechnol Adv 31, 945–961. https://doi.org/10.1016/j.biotechadv.2013.02.008

Lama, S., Kim, Y., Nguyen, D.T., Im, C.H., Sankaranarayanan, M., Park, S., 2021. Production of 3-hydroxypropionic acid from acetate using metabolically-engineered and glucose-grown Escherichia coli. Bioresour Technol 320, 124362. https://doi.org/10.1016/j.biortech.2020.124362

Lee, J.J.L., Ng, K.R., Liang, J., Cui, X., Li, A., Chen, W.N., 2022. Engineering the Phenylpropanoid Pathway in *Rhodosporidium toruloides* for Naringenin Production from Tyrosine by Leveraging on its Native *PAL* Gene. ACS Food Science & Technology. https://doi.org/10.1021/acsfoodscitech.2c00301

LI, Y., LIU, B., ZHAO, Z., BAI, F., 2006. Optimization of Culture Conditions for Lipid Production by Rhodosporidium toruloides. Chin J Biotechnol 22, 650–656. https://doi.org/10.1016/S1872-2075(06)60050-2

Li, Y., Wang, X., Ge, X., Tian, P., 2016. High Production of 3-Hydroxypropionic Acid in Klebsiella pneumoniae by Systematic Optimization of Glycerol Metabolism. Sci Rep 6, 26932. https://doi.org/10.1038/srep26932

Liu, C., Ding, Y., Zhang, R., Liu, H., Xian, M., Zhao, G., 2016. Functional balance between enzymes in malonyl-CoA pathway for 3-hydroxypropionate biosynthesis. Metab Eng 34, 104–111. https://doi.org/10.1016/j.ymben.2016.01.001

Liu, C., Wang, Q., Xian, M., Ding, Y., Zhao, G., 2013. Dissection of Malonyl-Coenzyme A Reductase of Chloroflexus aurantiacus Results in Enzyme Activity Improvement. PLoS One 8, e75554. https://doi.org/10.1371/journal.pone.0075554

Liu, D., Geiselman, G.M., Coradetti, S., Cheng, Y., Kirby, J., Prahl, J., Jacobson, O., Sundstrom, E.R., Tanjore, D., Skerker, J.M., Gladden, J., 2020. Exploiting nonionic surfactants to enhance fatty alcohol production in *Rhodosporidium toruloides*. Biotechnol Bioeng 117, 1418–1425. https://doi.org/10.1002/bit.27285

Liu, D., Xiao, Y., Evans, B.S., Zhang, F., 2015. Negative Feedback Regulation of Fatty Acid Production Based on a Malonyl-CoA Sensor–Actuator. ACS Synth Biol 4, 132–140. https://doi.org/10.1021/sb400158w

Liu, H., Zhao, X., Wang, F., Li, Y., Jiang, X., Ye, M., Zhao, Z.K., Zou, H., 2009. Comparative proteomic analysis of *Rhodosporidium toruloides* during lipid accumulation. Yeast 26, 553–566. https://doi.org/10.1002/yea.1706

Love, M.I., Huber, W., Anders, S., 2014. Moderated estimation of fold change and dispersion for RNA-seq data with DESeq2. Genome Biol 15. https://doi.org/10.1186/s13059-014-0550-8

Nguyen, N.H., Kim, J.-R., Park, S., 2019. Development of Biosensor for 3-Hydroxypropionic Acid. Biotechnology and Bioprocess Engineering 24, 109–118. https://doi.org/10.1007/s12257-018-0380-8

Nguyen-Vo, T.P., Ko, S., Ryu, H., Kim, J.R., Kim, D., Park, S., 2020. Systems evaluation reveals novel transporter YohJK renders 3-hydroxypropionate tolerance in Escherichia coli. Sci Rep 10, 19064. https://doi.org/10.1038/s41598-020-76120-3

Nguyen-Vo, T.P., Ryu, H., Sauer, M., Park, S., 2022. Improvement of 3-hydroxypropionic acid tolerance in Klebsiella pneumoniae by novel transporter YohJK. Bioresour Technol 346, 126613. https://doi.org/10.1016/j.biortech.2021.126613

Nora, L.C., Wehrs, M., Kim, J., Cheng, J.-F., Tarver, A., Simmons, B.A., Magnuson, J., Harmon-Smith, M., Silva-Rocha, R., Gladden, J.M., Mukhopadhyay, A., Skerker, J.M., Kirby, J., 2019. A toolset of constitutive promoters for metabolic engineering of Rhodosporidium toruloides. Microb Cell Fact 18, 117. https://doi.org/10.1186/s12934-019-1167-0

Osorio-González, C.S., Hegde, K., Ferreira, P., Brar, S.K., Kermanshahipour, A., Soccol, C.R., Avalos-Ramírez, A., 2019. Lipid production in Rhodosporidium toruloides using C-6 and C-5 wood hydrolysate: A comparative study. Biomass Bioenergy 130, 105355. https://doi.org/10.1016/j.biombioe.2019.105355

Otoupal, P.B., Ito, M., Arkin, A.P., Magnuson, J.K., Gladden, J.M., Skerker, J.M., 2019. Multiplexed CRISPR-Cas9-Based Genome Editing of *Rhodosporidium toruloides*. mSphere 4. https://doi.org/10.1128/mSphere.00099-19

Park, Y.-K., Nicaud, J.-M., Ledesma-Amaro, R., 2018. The Engineering Potential of Rhodosporidium toruloides as a Workhorse for Biotechnological Applications. Trends Biotechnol 36, 304–317. https://doi.org/10.1016/j.tibtech.2017.10.013

Pomraning, K.R., Dai, Z., Munoz, N., Kim, Y.-M., Gao, Y., Deng, S., Kim, J., Hofstad, B.A., Swita, M.S., Lemmon, T., Collett, J.R., Panisko, E.A., Webb-Robertson, B.-J.M., Zucker, J.D., Nicora, C.D., de Paoli, H., Baker, S.E., Burnum-Johnson, K.E., Hillson, N.J., Magnuson, J.K., 2021. Integration of Proteomics and Metabolomics Into the Design, Build, Test, Learn Cycle to Improve 3-Hydroxypropionic Acid Production in Aspergillus pseudoterreus. Front Bioeng Biotechnol 9. https://doi.org/10.3389/fbioe.2021.603832

Pomraning, K.R., Dai, Z., Munoz, N., Kim, Y.M., Gao, Y., Deng, S., Lemmon, T., Swita, M.S., Zucker, J.D., Kim, J., Mondo, S.J., Panisko, E., Burnet, M.C., Webb-Robertson, B.J.M., Hofstad, B., Baker, S.E., Burnum-Johnson, K.E., Magnuson, J.K., 2022. Itaconic acid production is regulated by LaeA in Aspergillus pseudoterreus. Metab Eng Commun 15. https://doi.org/10.1016/j.mec.2022.e00203

Qiao, K., Imam Abidi, S.H., Liu, H., Zhang, H., Chakraborty, S., Watson, N., Kumaran Ajikumar, P., Stephanopoulos, G., 2015. Engineering lipid overproduction in the oleaginous yeast Yarrowia lipolytica. Metab Eng 29, 56–65. https://doi.org/10.1016/j.ymben.2015.02.005

Rathnasingh, C., Raj, S.M., Lee, Y., Catherine, C., Ashok, S., Park, S., 2012. Production of 3-hydroxypropionic acid via malonyl-CoA pathway using recombinant Escherichia coli strains. J Biotechnol 157, 633–640. https://doi.org/10.1016/j.jbiotec.2011.06.008

Riscaldati, E., Moresi, M., Federici, F., Petruccioli, M., 2000. Effect of pH and stirring rate on itaconate production by Aspergillus terreus, Journal of Biotechnology.

Runguphan, W., Keasling, J.D., 2014. Metabolic engineering of Saccharomyces cerevisiae for production of fatty acid-derived biofuels and chemicals. Metab Eng 21, 103–113. https://doi.org/10.1016/j.ymben.2013.07.003

Sá-Pessoa, J., Paiva, S., Ribas, D., Silva, I.J., Viegas, S.C., Arraiano, C.M., Casal, M., 2013. SATP (YaaH), a succinate–acetate transporter protein in *Escherichia coli*. Biochemical Journal 454, 585–595. https://doi.org/10.1042/BJ20130412

Schultz, J.C., Cao, M., Zhao, H., 2019. Development of a CRISPR/Cas9 system for high efficiency multiplexed gene deletion in *Rhodosporidium toruloides*. Biotechnol Bioeng 116, 2103–2109. https://doi.org/10.1002/bit.27001

Schultz, J.C., Mishra, S., Gaither, E., Mejia, A., Dinh, H., Maranas, C., Zhao, H., 2022. Metabolic engineering of Rhodotorula toruloides IFO0880 improves C16 and C18 fatty alcohol production from synthetic media. Microb Cell Fact 21, 26. https://doi.org/10.1186/s12934-022-01750-3

Takayama, S., Ozaki, A., Konishi, R., Otomo, C., Kishida, M., Hirata, Y., Matsumoto, T., Tanaka, T., Kondo, A., 2018. Enhancing 3-hydroxypropionic acid production in combination with sugar supply engineering by cell surface-display and metabolic engineering of Schizosaccharomyces pombe. Microb Cell Fact 17, 176. https://doi.org/10.1186/s12934-018-1025-5

Vieira, N., Casal, M., Johansson, B., MacCallum, D.M., Brown, A.J.P., Paiva, S., 2010. Functional specialization and differential regulation of short-chain carboxylic acid transporters in the pathogen *Candida albicans*. Mol Microbiol 75, 1337–1354. https://doi.org/10.1111/j.1365-2958.2009.07003.x

Wang, J., Ledesma-Amaro, R., Wei, Y., Ji, B., Ji, X.-J., 2020. Metabolic engineering for increased lipid accumulation in Yarrowia lipolytica – A Review. Bioresour Technol 313, 123707. https://doi.org/10.1016/j.biortech.2020.123707

Wang, Y., Sun, T., Gao, X., Shi, M., Wu, L., Chen, L., Zhang, W., 2016. Biosynthesis of platform chemical 3-hydroxypropionic acid (3-HP) directly from CO2 in cyanobacterium Synechocystis sp. PCC 6803. Metab Eng 34, 60–70. https://doi.org/10.1016/j.ymben.2015.10.008

Wehrs, M., Gladden, J.M., Liu, Y., Platz, L., Prahl, J.-P., Moon, J., Papa, G., Sundstrom, E., Geiselman, G.M., Tanjore, D., Keasling, J.D., Pray, T.R., Simmons, B.A., Mukhopadhyay, A., 2019. Sustainable bioproduction of the blue pigment indigoidine: Expanding the range of heterologous products in *R. toruloides* to include non-ribosomal peptides. Green Chemistry 21, 3394–3406. https://doi.org/10.1039/C9GC00920E

Wen, Z., Zhang, S., Odoh, C.K., Jin, M., Zhao, Z.K., 2020. *Rhodosporidium toruloides* - A potential red yeast chassis for lipids and beyond. FEMS Yeast Res 20. https://doi.org/10.1093/femsyr/foaa038

Werpy, T., Petersen, G., 2004. Top Value Added Chemicals from Biomass: Volume I -- Results of Screening for Potential Candidates from Sugars and Synthesis Gas. Golden, CO (United States). https://doi.org/10.2172/15008859

Yaegashi, J., Kirby, J., Ito, M., Sun, J., Dutta, T., Mirsiaghi, M., Sundstrom, E.R., Rodriguez, A., Baidoo, E., Tanjore, D., Pray, T., Sale, K., Singh, S., Keasling, J.D., Simmons, B.A., Singer, S.W., Magnuson, J.K., Arkin, A.P., Skerker, J.M., Gladden, J.M., 2017. Rhodosporidium toruloides: a new platform organism for conversion of lignocellulose into terpene biofuels and bioproducts. Biotechnol Biofuels 10, 241. https://doi.org/10.1186/s13068-017-0927-5

Yang, Y.-M., Chen, W.-J., Yang, J., Zhou, Y.-M., Hu, B., Zhang, M., Zhu, L.-P., Wang, G.-Y., Yang, S., 2017a. Production of 3-hydroxypropionic acid in engineered Methylobacterium extorquens AM1 and its reassimilation through a reductive route. Microb Cell Fact 16, 179. https://doi.org/10.1186/s12934-017-0798-2

Yang, Y.-M., Chen, W.-J., Yang, J., Zhou, Y.-M., Hu, B., Zhang, M., Zhu, L.-P., Wang, G.-Y., Yang, S., 2017b. Production of 3-hydroxypropionic acid in engineered Methylobacterium extorquens AM1 and its reassimilation through a reductive route. Microb Cell Fact 16, 179. https://doi.org/10.1186/s12934-017-0798-2

Ye, Z., Sun, T., Hao, H., He, Y., Liu, X., Guo, M., Chen, G., 2021. Optimising nutrients in the culture medium of Rhodosporidium toruloides enhances lipids production. AMB Express 11, 149. https://doi.org/10.1186/s13568-021-01313-6

Zhang, S., Skerker, J.M., Rutter, C.D., Maurer, M.J., Arkin, A.P., Rao, C. v., 2016. Engineering *Rhodosporidium toruloides* for increased lipid production. Biotechnol Bioeng 113, 1056–1066. https://doi.org/10.1002/bit.25864

Zhang, Y., Nielsen, J., Liu, Z., 2021. Yeast based biorefineries for oleochemical production. Curr Opin Biotechnol 67, 26–34. https://doi.org/10.1016/j.copbio.2020.11.009

Zhao, Z., Liu, Y., Wang, F., Li, X., Deng, S., Xu, J., Wei, W., Wang, F., 2017. Life cycle assessment of primary energy demand and greenhouse gas (GHG) emissions of four propylene production pathways in China. J Clean Prod 163, 285–292. https://doi.org/10.1016/j.jclepro.2015.12.099

Zhou, S., Ashok, S., Ko, Y., Kim, D.M., Park, S., 2014. Development of a deletion mutant of Pseudomonas denitrificans that does not degrade 3-hydroxypropionic acid. Appl Microbiol Biotechnol 98, 4389–4398. https://doi.org/10.1007/s00253-014-5562-5

Zhou, S., Catherine, C., Rathnasingh, C., Somasundar, A., Park, S., 2013. Production of 3-Hydroxypropionic Acid From Glycerol by Recombinant Pseudomonas denitrificans. Biotechnol. Bioeng 110, 3177–3187. https://doi.org/10.1002/bit.24980/abstract

Zhu, Z., Zhang, S., Liu, H., Shen, H., Lin, X., Yang, F., Zhou, Y.J., Jin, G., Ye, M., Zou, H., Zhao, Z.K., 2012. A multi-omic map of the lipid-producing yeast Rhodosporidium toruloides. Nat Commun 3, 1112. https://doi.org/10.1038/ncomms2112